Thermal Performance Analysis of Small Hermetic Refrigeration and Air-Conditioning Compressors*

Man-Hoe KIM** and Clark W. BULLARD***

A simple physical model for small hermetic reciprocating, rotary and scroll compressors has been developed based on thermodynamic principles and large data sets from the compressor calorimeter and *in situ* tests. Pressure losses along the refrigerant path are neglected and a compression process is assumed isentropic. A mass flow rate model reflects clearance volumetric efficiency and simulates suction gas heating using an effectiveness method. Compressor work is calculated using the compressor efficiency represented by only two empirical parameters. A linear relationship between the discharge and shell temperatures is extracted from the large data sets and applied to the model for calculating the discharge temperature. Another experimental observation indicates that the specific volumes at the suction and discharge ports of the cylinder have linear relationships with the specific volumes at the compressor suction and discharge. Those relationships can be used for the compressor model and the possibility is reported. The models developed using physical principles and experimental observations can predict the mass flow rate and power consumption within ±3.0% accuracy.

Key Words: Hermetic Compressor, Thermal Performance, Compressor Model, Effectiveness, Compressor Efficiency

1. Introduction

The compressor is one of major components of an air-conditioning or refrigeration system and has an important effect on system energy efficiency. Compressor manufacturers usually provide empirical performance curves called compressor maps, expressing mass flow and power input as polynomial functions of evaporation temperature for a range of condensing temperatures. Since they are based on fixed ambient and suction gas temperatures, the maps are useful for comparing and selecting the compressors. However, they are inadequate for general system analysis, because they contain no information about the effects of different ambient and suction temperatures and are unable to predict discharge temperatures, which define the condenser inlet condition. Dabiri and Rice[1] suggested additional assumptions to account for suction gas heating, which have been used with limited success for reciprocating compressors with low-side sumps, and with greater success for rotary compressors where the suction gas is injected directly[2]. Haider et al.[3] investigated the effect of compressor map and ambient temperature on the power consumption of a refrigerator-freezer using the ERA (EPA Refrigerator Analysis) software, complemented by the measured compressor and refrigerator-freezer data. They reported the accuracy of ERA estimation could be improved up to 5.1% at an ambient temperature of 43.3°C by using the measured map data at 43.3°C rather than the given map at standard test condition of 32.2°C.

There are several detailed physical models of compressors in the literature. Prakash and Singh[4] developed a mathematical model for a reciprocating compressor using the first law of thermodynamics and assuming the refrigerant is an ideal gas. Hiller and Glicksmann[5] reported a detailed compressor model of reciprocating compressors and compared the simulation results with experimental data. Domanski and

* Received 15th April, 2002 (No. 02-5052)

** R & D Center, DA Network Business, Samsung Electronics Company, 416 Maetan-3Dong, Suwon, 442-742, Korea. E-mail: kimmh@asme.org

*** Department of Mechanical and Industrial Engineering, University of Illinois at Urbana-Champaign, 1206 West Green Street, Urbana, IL 61801, USA. E-mail: bullard@uiuc.edu

Didion[6] developed a quite detailed compressor model for a system simulation, but it requires over 30 input parameters. Todescat et al.[7] presented a thermal energy analysis of a reciprocating hermetic compressor using the energy balances for several parts of the compressor. They reported the effect of compressor shell temperature on the compressor performance such as power consumption and energy efficiency ratio. Recently, Cavallini et al.[8] presented a steady state model for the thermal analysis of a hermetic reciprocating compressor and compared with a few experimental data points for R-134a and R-600a compressors. Rigola et al.[9] presented an advanced numerical scheme of the thermal and fluid dynamic behavior of small hermetic reciprocating compressors, along with some empirical data. Those models usually require large sets of unknown parameters to characterize the complicated refrigerant flow, heat exchanges, effects of oil, and moving boundaries, plus data on the geometry and heat transfer characteristics of internal parts. Most such papers contain too little data to distinguish accurate parameter estimation from merely "tuning" the model for a few selected operating conditions. Jahnig et al.[10] developed a model similar to that presented here, which embodies different physical assumptions underlying the mass flow and power submodels.

The purpose of this paper is to establish a foundation for the development of a simple physical model of small hermetic compressors. It extends to rotary and scroll devices an approach explored first for small hermetic reciprocating compressors[11]. Instead of taking a detailed approach, the goal is to find the simplest formulation suitable for use in refrigerator and *a/c* simulation models. Pressure losses along the refrigerant path are neglected and the compression process is assumed as isentropic. A mass flow rate model reflects clearance volumetric efficiency and simulates suction gas heating using an effectiveness method. Compressor work is calculated using the compressor efficiency represented by only two empirical parameters. A linear relationship between the discharge and shell temperatures is extracted from the data and used for calculating the discharge temperature for any ambient air temperature.

2. Nomenclature

C : clearance volume ratio
h : specific enthalpy (J/kg)
$\dot{m}$: refrigerant mass flow rate (kg/h)
N : number of data points
P : pressure (kPa)
Q : heat transfer rate from shell (W)
s : specific entropy (kJ/kg °C)
T : temperature (°C)
UA : overall heat transfer coefficient (W/m² °C)
V_{disp} : cylinder displacement (m^3)
v : specific volume (m^3/kg)
W : compressor work (W)

Greek symbols

ε : effectiveness
η_c : compressor efficiency
η_v : volumetric efficiency
ω : compressor speed (rpm)

Subscripts

amb : ambient
cal : calculation
cond : condenser
dis : compressor shell discharge
dp : cylinder discharge port
evap : evaporator
exp : experimental
shell : compressor shell
sp : cylinder suction port
suc : compressor shell suction

3. Simple Physical Model

The basic purpose of the compressor sub-model in a larger system model is to provide the refrigerant mass flow rate, power consumption and discharge states of the compressor using some given information. The usual input data are compressor geometry (displacement and clearance volume), compressor speed, suction pressure and temperature, discharge pressure, and ambient temperature. The general compressor model is developed using large data sets available from calorimeter and *in situ* testing of reciprocating compressors. Table 1 shows the data sets to be used for the model.

3.1 Thermodynamic analysis

A detailed thermodynamic model of a compressor

Table 1 Data sets used for the model and computer simulations

data set	type of compressor	displacement/ clearance (cc)	Refrigerant	test methods	number of data points (N)
I	reciprocating	7.276/0.0606	R-134a	compressor calorimeter	30
II	reciprocating	7.276/0.0606	R-134a	*in situ* (refrigerator-freezer)	41
III	reciprocating	7.751/0.1550	R-12	*in situ* (refrigerator-freezer)	50
IV	rotary	7.391/0.0739	R-12	*in situ* (refrigerator-freezer)	35
V	scroll	27.354/ -	R-410A	*in situ* (split system air-conditioner)	34

is extremely complex due to the inherently complicated structure of the compressor and refrigerant flow pathways, along which heat transfer and pressure vary substantially and rapidly. For some applications (e.g. design of variable-speed drives) such detailed modeling is necessary[12]. Our hypothesis is that the requirements for quasi-steady system simulation modeling are much less demanding, so several assumptions can be made to simplify the physical model for small hermetic refrigeration and air-conditioning compressors:

(1) The refrigerant path can be treated as a steady state flow;

(2) The compression process is isentropic;

(3) The kinetic and potential energies of refrigerant are neglected;

(4) The pressure losses along the refrigerant path are neglected;

(5) The oil effects on the refrigerant properties are neglected.

Figure 1 shows a schematic diagram for typical low-side sump reciprocating and high-side sump rotary compressors. The following is a simple description for the refrigerant compression process of a low-side sump reciprocating compressor. Refrigerant vapor at low pressure and temperature enters the compressor shell through suction line and is heated as it cools the motor and other parts, and mixes with hot plenum gas along the refrigerant suction path. After compression in the cylinder, high temperature and pressure refrigerant gas discharges through a muffler, rejecting heat to the plenum gas before exiting via the discharge line. In case of high-side sump rotary compressor, refrigerant gas is directly introduced into the suction port of the cylinder through piping, and the compressed gas is directed into the compressor shell. Therefore, in case of the high-side sump compressors the entire compressor is at high discharge pressure, while for the low-side sump compressors most of the shell is at low suction pressure.

For a given compressor velocity and swept volume, the mass flow rate can be calculated using the volumetric efficiency[13].

$$\dot{m}=60\frac{\eta_v V_{disp}\omega}{v_{sp}} \qquad (1)$$

The volumetric efficiency for reciprocating and rotary compressors is given by Eq.(2), which accounts for re-expansion of the gas remaining in the clearance volume.

$$\eta_v=1-C\left(\frac{v_{sp}}{v(P_{dp}, s_{sp})}-1\right) \qquad (2)$$

The volumetric efficiency for a scroll compressor is difficult to quantify except by test, and so it is estimated from the test data (with $\alpha=0.013\,75$ and $\beta=1.746$).

$$\eta_v=1-\alpha\left(\frac{P_{dp}}{P_{sp}}\right)^{\beta} \qquad (3)$$

For a small hermetic compressor, we assume compression and re-expansion processes to be isentropic so the specific volume at the discharge port of the cylinder can be calculated. The decrease in density due to suction gas heating and mixing between the suction line to suction port has a large effect on the volumetric efficiency and mass flow rate. We assume that both the direct effect (suction gas contact with hot metal) and indirect effect (mixing with heated plenum gas) are driven by the same maximum temperature differential within the subsystem boundary between suction and discharge lines:

$$\varepsilon=\frac{h_{sp}-h_{suc}}{h(P_{sp}, T_{dp})-h_{suc}} \qquad (4)$$

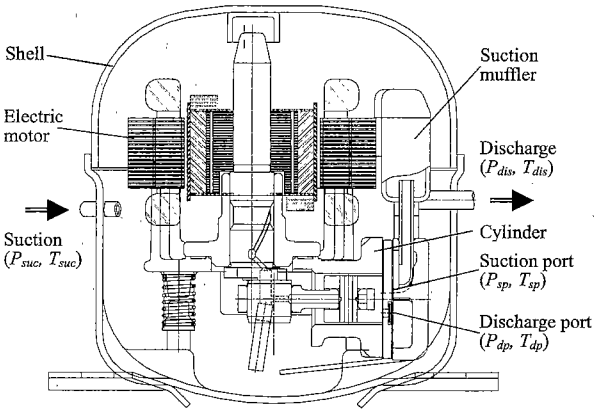

(a) Low-side sump reciprocating compressor

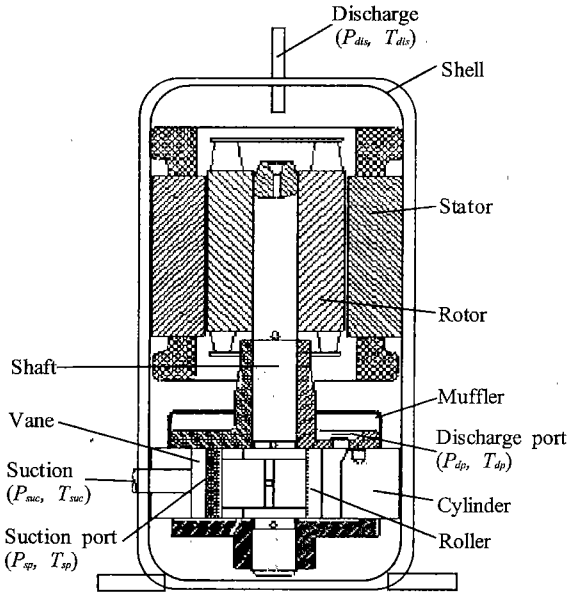

(b) High-side sump rolling piston rotary compressor

Fig. 1 Schematic diagram for small hermetic compressors

The maximum enthalpy at the suction port of the cylinder is determined using the suction port's pressure and the discharge port temperature, based on the assumption of isentropic compression. The effectiveness ε between the suction gas and the isothermal metal parts is assumed to be constant over the range of mass flow rates and is determined by minimizing the following objective function to obtain the best agreement with the measured mass flow rate at N data points.

$$obj\_\dot{m}=\min\sqrt{\frac{\sum_{n=1}^{N}\left(\frac{\dot{m}_{\exp}-\dot{m}_{cal}}{\dot{m}_{\exp}}\right)^2}{N}} \quad (5)$$

The compressor power consumption can be calculated if the compressor efficiency is known. The isentropic compressor efficiency is normally defined across the entire compressor shell, but in our case we define a compression efficiency that excludes the effects of subsystem heat transfers upstream of the suction port, and includes the effects of motor efficiency:

$$\eta_c=\dot{m}[h(P_{dp}, s_{sp})-h_{sp}]/W \quad (6)$$

Empirical observation shows that the compressor efficiency can be expressed simply as:

$$\eta_c=k_1+k_2T_{shell} \quad (7)$$

where the constants k_1 and k_2 can be estimated by minimizing the average normalized deviation between measured and calculated power consumption.

$$obj\_W=\min\sqrt{\frac{\sum_{n=1}^{N}\left(\frac{W_{\exp}-W_{cal}}{W_{\exp}}\right)^2}{N}} \quad (8)$$

The empirically observed dependence of compression efficiency on shell temperature is thought to reflect the temperature dependence of oil viscosity. The principal mechanism of oil cooling, splattering into the compressor shell, determines the relationship between shell temperature and oil temperature.

Three more parameters are needed to estimate the discharge temperature. The first step is to apply the first law of thermodynamics across the compressor shell using the following equation for the steady state flow, neglecting the potential and kinetic energy.

$$Q=W-\dot{m}(h_{dis}-h_{suc}) \quad (9)$$

Our experimental observations, over a wide range of operating conditions with multiple thermocouples attached to the compressor shell, suggested a linear relationship with the discharge temperature

$$T_{shell}=a+bT_{dis} \quad (10)$$

where, a and b are empirical constants determined from at least two experimental data points.

Finally, the heat transfer from the compressor shell can be obtained from the equation

$$Q=UA_{shell}(T_{shell}-T_{amb}) \quad (11)$$

If discharge temperatures are available for more operating conditions, UA_{shell} is a constant to be determined using the least square method with the measured heat loss values

$$obj\_Q=\min\sqrt{\frac{\sum_{n=1}^{N}\left(\frac{Q_{\exp}-Q_{cal}}{Q_{\exp}}\right)^2}{N}} \quad (12)$$

A Newton-Raphson based equation solver[14] was used for both the simulation and optimization calculations needed to estimate these parameters.

3.2 Simulation and parameter estimation results

Table 1 shows five data sets used in this study. For the first compressor type (R134a refrigerator compressor) data set I consists of 30 data points from manufacturer's calorimeter tests conducted on a prototype at 43.3°C ambient over a wide range of suction and discharge pressures. Data set II is for a different [production] compressor, but the same model. It consists of 41 data points from *in situ* testing of a refrigerator instrumented with immersion thermocouples, obtained by Srichai and Bullard[15] and Kelman and Bullard[16] over wide range of suction (12.8 - 37.8°C) and ambient temperatures (21.1 - 45.6°C). The given displacements and clearance volumes for each compressor are 7.276 cc and 0.060 6 cc, respectively and the nominal compressor speed is 3 450 rpm. Data set III was obtained *in situ* under a similar range of conditions using an older R12 compressor of similar design. Data set IV for a R12 rotary compressor and data set V for a R410A low-side sump scroll compressor were also obtained from *in situ* testing of a refrigerator-freezer and a split system air-conditioner, respectively. In latter three cases however, the compressor displacement, clearance volume and rpm were unknown, so those values were estimated simultaneously using the suction heat transfer effectiveness at compressor speed: 3 450 rpm as shown in Table 1.

The simulation results are depicted in Figs. 2 - 6, compared with measured values. Table 2 shows the estimated parameters and rms errors of simulation results for each data set. The parameter estimates were obtained using the complete data sets; the small standard deviations apparent from Figs. 2 - 6 indicate that smaller subsets of data could yield similar results. The calculated mass flow rates and power inputs are in good agreement with measured values, especially considering measurement accuracy. The estimate for heat transfer effectiveness of the suction gas was nearly identical for the prototype and production R134a compressors. The lower accuracy of the manufacturer's data set I compared to the *in situ* data set II may be due to inaccurate measurements of suction and discharge temperatures, since manufacturers use surface thermocouples that could be affected via conduction by the compressor shell. Mass

Table 2 Estimated parameters and rms errors for the physical model

Data set	Estimated constants						rms errors		
							%		°C
	ε	k_1	k_2	a	b	UA_{shell}	obj_mr	obj_W	ΔT_{dis}
I	0.242	0.240	0.00619	28.72	0.441	59.96	2.58	2.37	2.3
II	0.293	0.417	0.00337	-2.16	0.818	34.52	0.92	1.10	0.6
III	0.596	0.285	0.00500	-18.80	0.822	78.42	0.73	1.69	3.2
IV	0.150	0.431	0.00178	-8.94	0.923	29.19	3.00	1.67	0.9
V	0.337	0.714	-0.00013	2.07	0.488	0.18	2.09	2.48	0.8

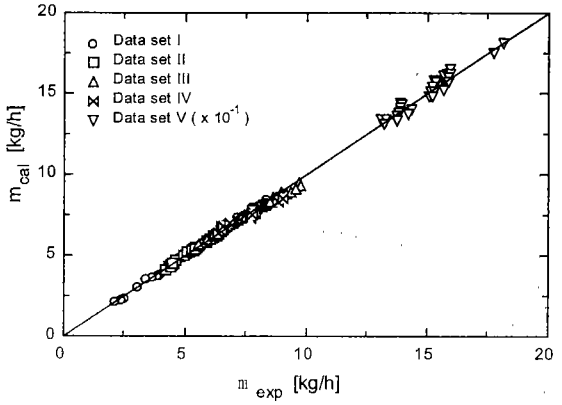

Fig. 2 Calculated and measured mass flow rates

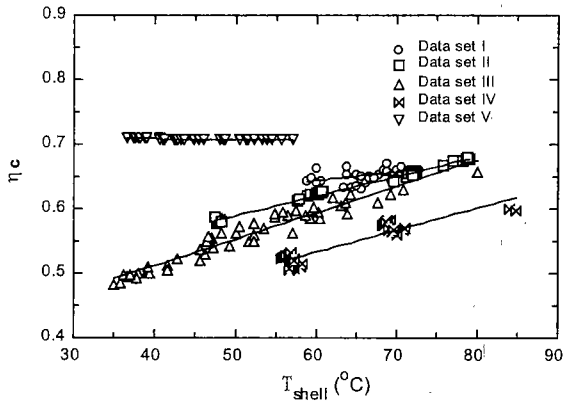

Fig. 3 Compressor efficiency as a function of shell temperature

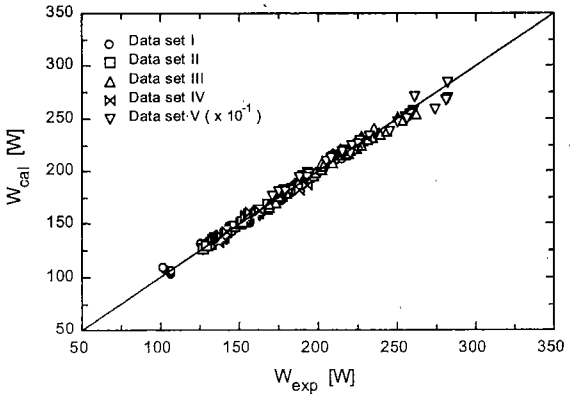

Fig. 4 Calculated and measured compressor powers

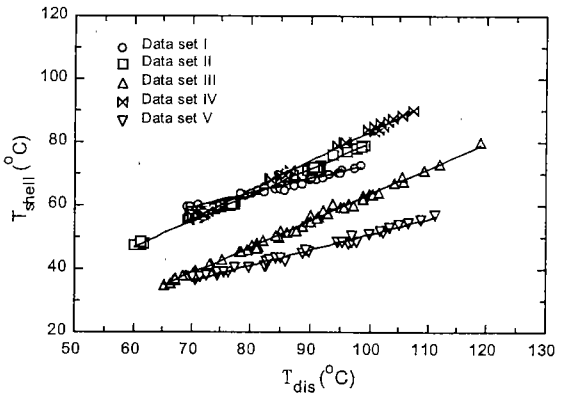

Fig. 5 Compressor shell temperature as a function of discharge temperature

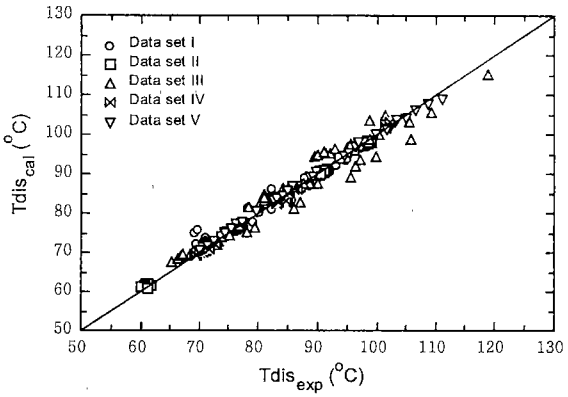

Fig. 6 Calculated and measured discharge temperatures

flow calculations were surprisingly accurate for data set III, despite the fact that displacement and clearance volumes were unknown and had to be estimated simultaneously with suction gas heat transfer effectiveness using Eq.(5). For a high-side-sump rotary compressor and a low-side-sump scroll compressor, the calculation results for the mass flow rate and compressor power showed reasonable accuracy and therefore the same physical model can be used.

Figure 5 demonstrates the linearity of the empirical correlation between the compressor shell and discharge temperatures. It is equally strong for the manufacturers' calorimeter testing performed at ambient temperature of 43.3°C, and the *in situ* data obtained over a wide range of air temperatures. This relation is used for estimating the discharge tempera-

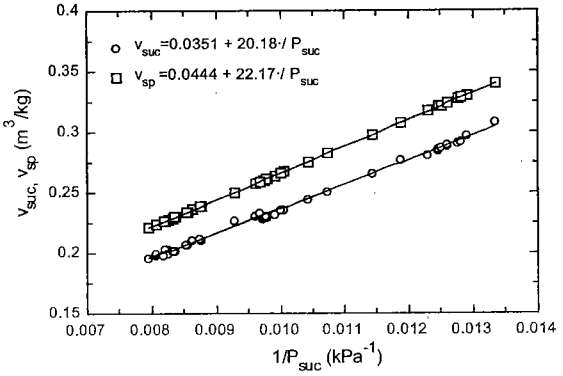

(a) Data set II (low-side sump)

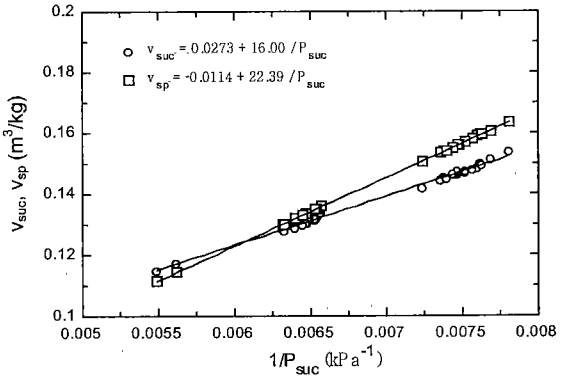

(b) Data set IV (high-side sump)

Fig. 7 Suction and suction port specific volumes as a function of the suction pressure

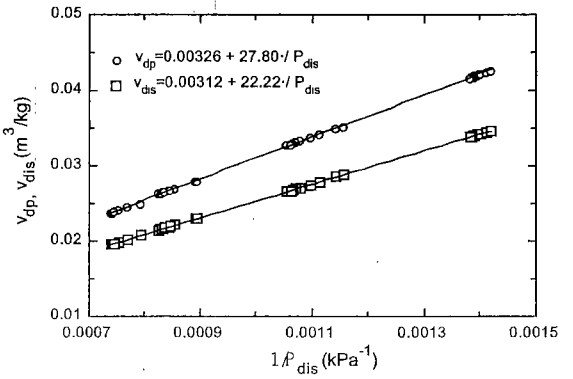

(a) Data set II (low-side sump)

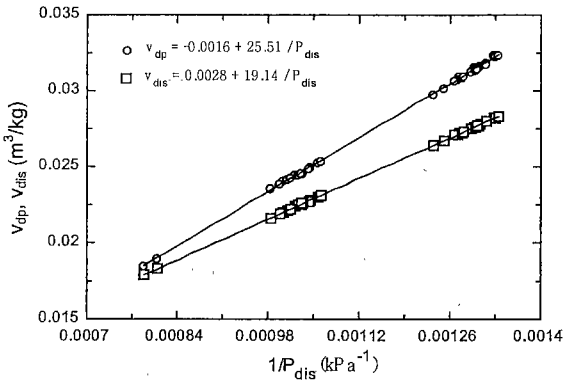

(b) Data set IV (high-side sump)

Fig. 8 Discharge and discharge port specific volumes as a function of the discharge pressure

ture and the overall heat transfer coefficient, UA_{shell}, of the compressor shell using Eq. (12). The estimated values of all the parameters affect the calculated discharge temperatures, which are compared to measured data in Table 2. For data set III, a larger scatter in shell heat transfer can be seen in the discharge temperature calculation. That particular refrigerator's air circulation pattern was rather complex (intake and exit both through the front grille) and about 30% of exit air was recirculated. After the experiment was complete, it was noted that the measurement of air temperature was very sensitive to the location of the thermocouple between the propeller fan and the compressor. The fan apparently failed to eliminate horizontal temperature gradient caused by recirculation, and vertical variation due to subcooling in the multislab condenser upstream of the fan. Finally the result for data set I illustrates the fact that errors in mass flow rate propagate directly into the power calculation (Eq. (8)), but tend to be compensated by the subsequent estimation of UA_{shell} to conform to the additional data on discharge temperature. Again, the higher accuracy of discharge temperature calculations for data set II vs. data set I may be attributable to the use of immersion thermocouples for measuring suction and discharge temperatures. These data from immersion thermocouples is useful because they provide support for the modeling assumptions employed, but in practice uninsulated surface thermocouples will probably continue to be used by manufacturers in compressor calorimeters. For a scroll compressor, very little heat transfer occurs between the shell and the ambient because the shell temperatures are relatively lower and compressor efficiency is higher than other compressors as shown in Fig. 3.

4. Empirical Relations

Another set of interesting empirical relations, shown in Figs. 7 and 8 for low-side sump (data set II) and high-side sump (data set IV), were obtained using least squares from the mass flows and discharge temperatures.

For small hermetic compressors considered here

$$v_{suc}=c_1+\frac{c_2}{P_{suc}} \tag{13}$$

$$v_{sp}=c_3+\frac{c_4}{P_{suc}} \tag{14}$$

$$v_{dp}=d_1+\frac{d_2}{P_{dis}} \tag{15}$$

Table 3 Estimated parameters and rms errors for the empirical model

Data set	Estimated constants						rms errors		
							%		°C
	k_3	k_4	c_3	c_4	d_3	d_4	obj_mr	obj_W	ΔT_{dis}
I	0.089	0.00668	-0.00724	28.70	-0.00247	27.98	2.95	2.11	8.0
II	0.417	0.00266	0.04439	22.17	0.00312	22.22	1.11	1.32	0.6
III	0.224	0.00376	0.03858	25.05	0.00282	19.27	1.60	1.45	2.3
IV	0.442	0.00130	-0.01136	22.39	0.00279	19.14	1.21	1.45	0.9
V	0.811	-0.00113	-0.00056	32.82	0.00148	28.55	0.32	1.70	3.2

$$v_{dis}=d_3+\frac{d_4}{P_{dis}} \tag{16}$$

where constants are presented in Table 3.

Rearranging the Eqs.(13) - (16) shows relationships between the specific volumes for the suction and discharge ports

$$v_{sp}=a_1+a_2 v_{suc} \tag{17}$$

$$v_{dp}=b_1+b_2 v_{dis} \tag{18}$$

where the constants can be estimated directly from the same experimental data. Equations(13) - (18) can be used for all the types of compressors considered in this study.

In the mass flow submodel, the two-parameter Eq.(14) or (17) can be used instead of the effectiveness Eq.(4) to determine the specific volume at the cylinder's suction port, quite accurately as shown in Table 3. The two-parameter Eq.(16) or (18) can be used for calculating discharge temperature, instead of the three parameter (a, b, UA_{shell}) used in the physical model. However, in this case, we can estimate compressor efficiency as a function of T_{dis} instead of T_{shell}, which was used in Eq.(7).

$$\eta_c=k_3+k_4 T_{dis} \tag{19}$$

The rms errors for mass flow rate and compressor power of the empirical model are within ±3.0%. However, shell heat loss and discharge temperature for the data set I show relatively large rms errors and those may be partly caused by the inaccuracy of the measured discharge temperatures and pressures.

5. Conclusions

A simple and general compressor (reciprocating, rotary, and scroll-type) model has been developed using the thermodynamic principles and large data sets from the compressor calorimeter and *in situ* tests. The model consists of three sequential steps: (1) mass flow rate (m); (2) compressor work (W); and (3) compressor shell heat transfer (Q) and discharge temperature (T_{dis}). The model can estimate mass flow rate and compressor power consumption with rms errors less than ±3.0%, which is not much larger than measurement errors associated with calorimeter testing under ideal conditions. The magnitude of the errors suggests that the six parameters could be estimated from data sets much smaller than those used here. The density decrease due to suction gas heating and mixing is a very important factor affecting mass flow rate, and can be characterized by a single parameter: the effectiveness of heat transfer driven by the difference between the temperatures at the suction line and the discharge port. Oil viscosity appears to be the most important factor accounting for compressor power consumption more than the isentropic ideal.

Fewer tests should be needed in calorimeter to estimate these six physical parameters, compared to the 18 - 20 parameters needed for today's polynomial curve fits of mass flow and power. However this approach requires that T_{shell} and T_{dis} should be recorded for at least two operating conditions during the calorimeter tests, in order to define the simple linear relation between them and to estimate the compressor shell heat transfer coefficient. Similarly, only two such data points would need to be obtained by OEM's to characterize accurately the compressor shell heat transfer coefficient in unique installations, where the air temperature at the compressor is influenced by the location of the condenser.

Acknowledgements

This work was supported by the 30 member companies of the Air Conditioning and Refrigeration Center (ACRC) at the University of Illinois at Urbana-Champaign.

References

(1) Dabiri, A.E. and Rice, C.K., A Compressor Simulation Model with Corrections for the Level of Suction Gas Superheat, ASHRAE Trans., Vol. 87, Pt. 2 (1981), pp. 771-782.

(2) Mullen, C.E., Bridges, B.D., Porter, K.J., Hahn, G.W. and Bullard, C.W., Development and Validation of a Room Air Conditioning Simulation Model, ASHRAE Transactions, Vol. 104, Pt. 2 (1988), pp. 389-397.

(3) Haider, I., Lavannis, M.K. and Radermacher, R., Investigations of the EPA Refrigerator Analysis (ERA) Software: Compressor Map and Ambient Temperature Effects, ASHRAE Transactions, Vol. 103, Pt. 11 (1997), pp. 608-618.

(4) Prakash, R. and Singh, R., Mathematical Model-

ing and Simulation of Refrigerating Compressors, Proceedings of the 1974 Purdue Compressor Technology Conference, (1974), pp. 274-285.
(5) Hiller, C.C. and Glicksman, L.R., Detailed Modeling and Computer Simulation of Reciprocating Refrigeration Compressors, Proceedings of the 1976 Purdue Compressor Technology Conference, (1976), pp. 12-17.
(6) Domanski, P.A. and Didion, D.A., Computer Modeling of the Vapor Compression Cycle with Constant Flow Area Expansion Device, National Bureau of Standards, Building Science Series, No. 155 (1983).
(7) Todescat, M.L., Fagotti, F., Prata, A.T. and Ferrerira, R.T.S., Thermal Energy Analysis in Reciprocating Hermetic Compressors, Proceedings of the 1992 International Compressor Engineering Conference at Purdue, (1992), pp. 1419-1428.
(8) Cavallini, A., Doretti, L., Longo, G.A., Rossetto, L., Bella, B. and Zannerio, A., Thermal Analysis of a Hermetic Reciprocating Compressor, Proceedings of the 1996 International Compressor Conference, Purdue University, West Lafayette, Indiana, (1996), pp. 535-540.
(9) Rigola, J., Perez-Segarra, C.D., Oliva, A., Serra, J.M., Escriba, M. and Pons, J., Parametric Study and Experimental Comparison of Small Hermetic Refrigeration Compressors Using an Advanced Numerical Simulation Model, Proceedings of the 1996 International Compressor Engineering Conference at Purdue, (1996), pp. 529-534.
(10) Jahnig, D.I., Reindl, D.T. and Klein, S.A., A Semi-Empirical Method for Representing Domestic Refrigerator/Freezer Compressor Calorimeter Test Data, ASHRAE Trans., Vol. 106, Pt. 2 (2000), pp. 122-130.
(11) Kim, M.-H. and Bullard, C.W., A Simple Approach to Thermal Performance Analysis of Small Hermetic Reciprocating Compressors, ASHRAE Trans., Vol. 107, Pt. 1 (2001), pp. 109-119.
(12) Rasmussen, B.D., Variable Speed Hermetic Reciprocating Compressors for Domestic Refrigerators, Ph.D. Thesis, Technical University of Denmark, (1997).
(13) Kuehn, T.M., Ramsey, J.W. and Threlkeld, J.L., Thermal Environmental Engineering, 3rd edition, (1998), Prentice Hall.
(14) Klein, S.A. and Alvarado, F.L., Engineering Equation Solver, version 5.029, (1999), F-Chart Software.
(15) Srichai, P.R. and Bullard, C.W., Two-Speed Compressor Operation in a Refrigerator/Freezer, ACRC TR-121, (1997), University of Illinois at Urbana-Champaign.
(16) Kelman, S. and Bullard, C.W., Dual Temperature Evaporator Refrigerator Design and Optimization, ACRC TR-148, (1999), University of Illinois at Urbana-Champaign.